



The Synergy of Dark Energy Probes

Andy Taylor & Tom Kitching

Institute for Astronomy, University of Edinburgh, Royal Observatory, Blackford Hill, Edinburgh, EH9 3HJ, United Kingdom
email: ant@roe.ac.uk, tdk@roe.ac.uk

Abstract. The nature of the dark energy dominating the energy budget of the Universe and driving the observed acceleration of its expansion is a major challenge for Cosmology. Here we discuss the observational signatures of dark energy and outline a number of promising approaches to determining its nature, including the Cosmic Microwave Background from Planck, gravitational lensing from darkCAM or DES, and Baryon Acoustic Oscillations from WFMOS. We use a Fisher Information Matrix formalism to predict the level of accuracy of each method for the dark energy equation of state and its evolution using the parametrization $w(a) = w_0 + w_a(1-a)$, in an 11-parameter cosmological model. The combination of probes is studied and the cumulative accuracy estimated. We find a limit of $\Delta w_0 = 0.025$ and $\Delta w_a = 0.078$ from these studies, or $\Delta w(z_p) = 0.013$ at a pivot redshift of $z_p = 0.4$. The accuracy of dark energy measurements is found to be data-limited for the foreseeable future.

1. Introduction

The observed acceleration of the the Universe (Reiss et al. 1998), its spatial flatness (Spergel et al. 2006) and low mass-density (Spergel et al. 2006; Sanchez et al. 2005) all point towards a dominant, negative-pressure “dark energy” component with an effective equation of state $p = w\rho$, with $w < -1/3$. The dark energy affects the evolution of the cosmic expansion factor of the Universe, $a(t) = (1+z)^{-1}$, and so the evolution of the Hubble parameter, $H(a)$. In turn this will affect distances measured by the photon equation of motion as a function of redshift, $r(z)$, and angular distances, $S_k(r) = \sin r$, r , or $\sinh r$ which also depend on the spatial curvature of the Universe. The growth of matter perturbations, $\delta(t)$, will be slowed or terminated by the accelerated expansion.

A physical explanation for the dark energy is a major challenge for Cosmology and fundamental Physics. We may divide potential solutions into classes where the dark energy arises from new particle physics, perhaps a new scalar field such as a quintessence, K-essence, or a tachyonic field; new gravitational physics due to extra dimensions or higher-order terms in the gravitational Lagrangian; a cosmological constant, Λ , which we may have to appeal to a multiverse scenario to explain; or more pedestrian physics where the acceleration is due to the nonlinear backreaction of structure on the photon path, although it is perhaps hard to see how this can account for all of the observations leading to dark energy.

The dark energy effective equation of state can be parameterized by

$$w(a) = w_0 + w_a(1-a) \quad (1)$$

where w_0 is the equation of state at $z = 0$, which grows to $w_0 + w_a$ for $z > 1$. This parameterization is not unique, or even physically motivated, but one hopes this model encapsulates a wide range of physical models. However

there will be a sector of models where this parameterization may not be adequate, such as non-Einstein gravity models. However, here we want to gain some insight as to where information on dark energy can come from, how to quantify this, and how different probes interact.

2. Dark Energy Probes

The accuracy with which a cosmological survey can probe dark energy can be estimated using the Fisher Information Matrix formalism (see e.g. Tegmark et al. 1997). We shall assume that the data, \mathbf{x} , is Gaussian distributed, or has Gaussian distributed noise properties, with a mean $\langle \mathbf{x} \rangle = \boldsymbol{\mu}$ and covariance matrix, $\mathbf{C} = \langle \mathbf{x}\mathbf{x}^t \rangle$. The expected accuracy with which model parameters, $\boldsymbol{\theta}$, for the data can be extracted can be estimated by

$$\langle \Delta\theta_i \Delta\theta_j \rangle = [\text{Tr} (\langle \Delta\mathbf{C}\Delta\mathbf{C} \rangle^{-1} \partial_i \mathbf{C} \partial_j \mathbf{C} + 2\mathbf{C}^{-1} \partial_i \boldsymbol{\mu} \partial_j \boldsymbol{\mu}^t)]^{-1}, \quad (2)$$

where $\langle \Delta\mathbf{C}\Delta\mathbf{C} \rangle = 2\mathbf{C}\mathbf{C}$ is the covariance matrix for a measurement of \mathbf{C} , and ∂_i is the gradient in parameter-space with respect to the i^{th} parameter. The Fisher approach assumes the likelihood surface in parameter space is Gaussian with elliptical error contours. The parameter errors on the diagonal of the covariance matrix are fully marginalized over all other parameters.

We shall assume a fiducial cosmological model with 11 parameters for the parameter vector, $\boldsymbol{\theta} = (\Omega_v, \Omega_m, \Omega_b, h, \sigma_8, \tau, n_s, \alpha_n, r, w_0, w_a)$, where τ is the CMB optical depth, $\alpha_n = dn_s/d \ln k$ is the running of the matter power spectrum index, and $r = T/S$ is the primordial tensor-to-scalar perturbation ratio. This allows for spatial curvature, which is degenerate with the dark energy. Our fiducial model parameters are from WMAP3 (Spergel et al. 2006), with values $\boldsymbol{\theta}_0 = (0.7, 0.3, 0.05, 0.72, 0.8, 0.1, 0.95, 0.0, 0.01, -1.0, 0.0)$.

We shall only quote results for the dark energy parameters, (w_0, w_a) , marginalizing over all other parameters. The data-sets we consider are expected results from the Planck CMB Surveyor, a weak gravitational lensing and photometric redshift survey such as darkCAM or the Dark Energy Survey, and a Baryon Acoustic Oscillation experiment such as WFMOS. We briefly outline each survey.

2.1. Planck CMB Surveyor

The primary CMB temperature and polarization signal, a snap-shot of the plasma-filled Universe at $z = 1100$, contains very little information on dark energy. The dark energy dependence arises from secondary effects such as the Integrated Sachs-Wolfe effect and gravitational lens distortions. Here we model a 14-month Planck CMB experiment, surveying 66% of the sky in temperature (T) and polarization (E & B). We sum over the angular power spectrum, $C_{\ell\ell'mm'}^X = (C_\ell^X + N_\ell^X)\delta_{\ell\ell'}^k\delta_{mm'}^K$, which is the signal-plus-noise angular power for the $X = (TT, TE, EE, BB)$ spectra, from $\ell = 10$ to 2000.

2.2. Weak Gravitational Lensing

Gravitational lensing depends on both the geometry of the observer, lens and source image, and the strength of the lens. Hence it can probe both the geometry and evolution of the growth of structure. With redshift information these effects can be disentangled (Taylor et al. 2004). We shall call the combination of weak lensing and photometric redshifts 3-D weak lensing.

i) 3-D Shear Power: The growth of matter perturbations and geometry can be probed in two ways by 3-D weak lensing (see Kitching page 97). Firstly one can form two-point statistics from the shear, for example the shear power spectra (e.g. Heavens 2003; Heavens et al. 2006) which depends on angular wavenumber and redshift, $C_\ell^{\gamma\gamma}(z, z')$. This depends on both the growth of structure and geometry.

ii) 3-D Shear-ratios: The second approach is to take shear ratios (e.g. Jain & Taylor 2003; Taylor et al. 2006). This removes the dependence on the mass of the lens, and hence on structure. The shear power probes the large-angle, weak-shear field, while the shear ratios measurement probes the stronger shear field behind clusters. In both estimates we take into account the effect of photometric redshift errors, sample and cosmic variance and shot noise due to the intrinsic ellipticity of galaxies.

For this analysis we assume we have a 10,000 sq. deg. photometric redshift survey with 5-band resolution of $\Delta z = 0.05(1+z)$, to a median depth of $z_m = 0.7$, containing the shear values for some 3×10^8 galaxies. We have assumed that the shear power measurements and shear ratios are independent. This is a reasonable assumption, since the 3-D shear power spectra probe the weak shear field on large-scales, while the shear-ratio analysis probes the shear field behind clusters and groups. In addition, the

shear ratio method factors out any dependence on structure, except in its noise terms.

2.3. Baryon Acoustic Oscillations

Dark energy can be probed by the Baryon Acoustic Oscillations (BAOs) in the galaxy power spectrum (Blake & Glazebrook 2003) as a standard ruler as a function of redshift or compared with the CMB. This again just probes the photon path, $r(z)$, and so is a purely geometric method. Here we shall include information about the shape of the galaxy power spectrum, but marginalize over its amplitude. This removes any dependence on a scale-independent galaxy bias parameter.

The survey we use for the BAO test is a WFMOS-like survey (e.g. Blake & Glazebrook 2003), with two redshift slices at $z = 1$ and $z = 3$, covering 5000 sq. deg. in the first slice and 300 sq. deg. in the higher redshift slice. We assume we have some 2×10^6 galaxies in the sample, all with good spectroscopic redshifts.

3. Synergy Between Dark Energy Probes

3.1. Fisher Analysis

Figure 1 shows the 2-parameter, 1- σ (68.3% confidence) likelihood contours for the dark energy parameters w_0 and w_a for the CMB, gravitational lensing shear power and shear ratios, and BAO experiments, having marginalized over all other parameters. Here we see that none of these experiments on their own strongly constrain the dark energy properties. This is due to degeneracies with other cosmological parameters, for instance spatial curvature. However, these experiments do slice out thin planes in the full 11-dimensional parameter space which are orthogonal. By combining experiments these planes will intersect in higher dimensions, breaking the degeneracies. When we combine these multi-dimensional ellipses, the intersection points can be much smaller than the original ellipses. One-parameter errors for combined surveys are also shown.

The angle of orientation of the error ellipses correspond to the redshift at which the dark energy measurement is most accurately probed. The lowest redshifts are probed by the shear ratio measurements (common ellipse in right-hand column), which is very insensitive to w_a . Next is the shear-power measurement (the ellipses in the top row) which probes both structure growth and geometry to constrain dark energy. At slightly higher-redshifts is the CMB estimation (common ellipses on the main diagonal) arising due to the Sachs-Wolfe effect and gravitational lensing. Finally, the BAO experiment (middle top, middle diagonal and middle right-hand column) is probing dark energy at higher redshifts, close to the lower-redshift bin.

3.2. Decoherence at Pivot Redshifts

While the w_0 - w_a parameterization of the equation of state is simple and hopefully summarizes a large range of dark

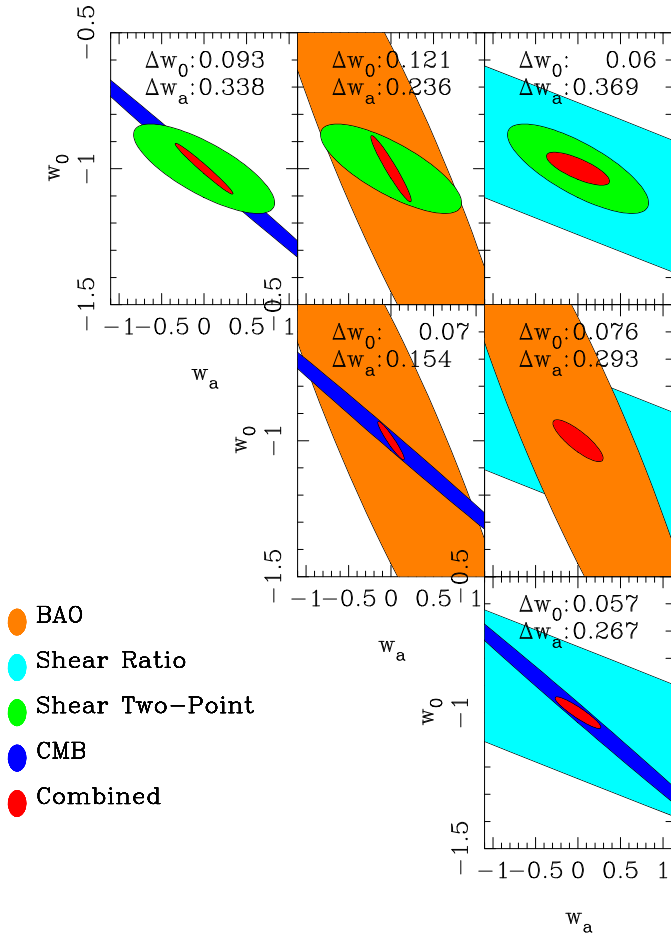


Fig. 1. The two parameter, $1-\sigma$ (68%) contours in the (w_0, w_a) plane marginalized over all other parameters, for the 3-D shear power (light ellipses along top panels), the 3-D geometric shear-ratio (light block in the left hand column), the 14-month Planck CMB Surveyor (dark strip in the central diagonal panels), a WFMOs-like BAO experiment (strip in the middle top, middle diagonal and middle right column), and the combined constraints (central ellipses in all panels).

energy models, it is harder to use it to quantify the overall constraint in the parameter space due to degeneracies between these parameters. To fully quantify the information we need to quote three numbers, Δw_0 , Δw_a , and the correlation coefficient of w_0 and w_a : $r(w_0, w_a)$. A more insightful re-parameterization is to expand the equation of state parameter around the scale factor at a decoherence, or pivot, redshift, z_p ;

$$w(a) = w_p + w_a(a_p - a), \quad (3)$$

where $w_p = w_0 + w_a(1 - a_p)$ and w_a become independent. The dark energy equation of state can now be fully specified by w_p , w_a and z_p .

Since w_p and w_a are independent variables by design, we can define a useful “Figure-of-Merit” by the area enclosed by the error ellipse in the w_p - w_a parameter space;

$$FoM = \Delta w_p \times \Delta w_a. \quad (4)$$

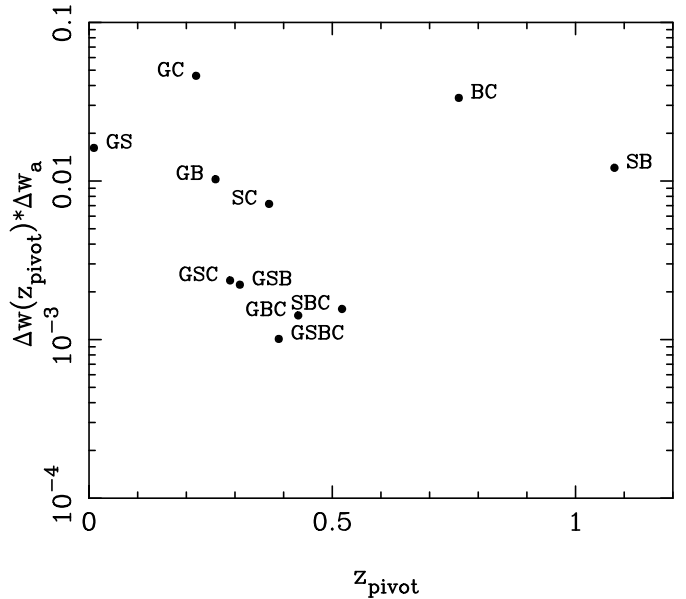


Fig. 2. The dark energy Figure-of-Merit versus the pivot redshift. The different dark energy probes shown are G = Geometric shear-ratios, S = Shear power, B = BAO, C = CMB. The survey parameters are given in Section 2.

Figure 2 shows the dark energy figure of merit estimated for the geometric shear-ratio method (G), the 3-D weak shear-power spectra analysis (S), the analysis of Baryonic Acoustic Oscillations (B), and the CMB (C). Survey details are given in Section 2. It is clear that the shear-ratio measurement probes low-redshifts, due to its weak dependence on w_a , while the BAO experiment probes the highest redshift, in agreement with our interpretation of Fig. 1. Combining probes considerably reduces the figure of merit and hence increases the accuracy with which the dark energy is pinned down. This process averages over the redshift range of the probes. For instance, the combination GSBC can be broken down into the survey pairs GS+BC, GC+SB and GB+SC, which are each a factor of 10 worse in terms of the figure of merit. However, the measurement of these individual pairs will allow the dark energy to be probed to similar accuracy at different redshifts, allowing for consistency checks.

Different methods also probe either just the global geometry of the Universe (shear-ratios, BAO’s) or the geometry and evolution of structure (shear-power and CMB). If the dark energy can be understood in terms of an effective equation of state, one would expect these probes and their combinations (GB and SC in Fig. 2) to agree. Differences could be due to the effective equation of state breaking down, such as in a non-Einstein gravity scenario.

Finally, Fig. 2 also illustrates a limitation in probing dark energy – how can we push the analysis of dark energy to higher redshifts? The highest redshift probes are the combination of 3-D shear-power and a BAO experiment, which probes the dark energy at $z = 1.08$, but only with $\Delta w_p \Delta w_a = 1.1 \times 10^{-2}$, compared to $\Delta w_p \Delta w_a = 1.0 \times 10^{-3}$ at $z = 0.4$ for all four surveys combined. With the

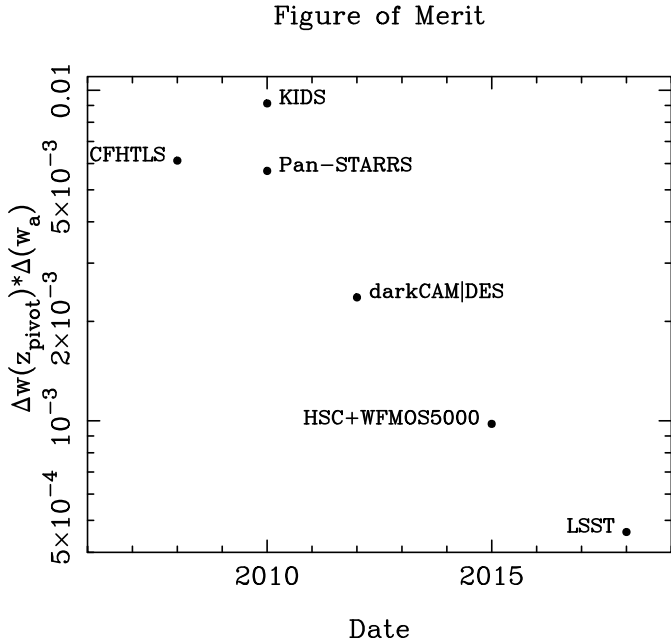


Fig. 3. The potential increase in knowledge of the dark energy parameters, w_p and w_a , as measured by the Figure-of-Merit, as a function of proposed survey completion date.

effects of dark energy diminishing with increasing redshift, and combining probes pushing the redshift probed down, how can we probe dark energy beyond $z = 1$?

4. Current and Future Ground-Based Surveys

The previous discussion was concerned with estimating the accuracy which combinations of dark energy surveys can achieve. But in practise not all of these experiments will be available at the same time. Here we try and estimate how our knowledge of the dark energy parameters may evolve over time, with the increase in size of proposed surveys. This is clearly of some interest. If our knowledge of dark energy is not data-limited, but instead limited by the diminishing effect of dark energy on the Universe at higher redshift, it is possible that we could find diminishing returns from larger surveys as dark energy effects saturate. This may lead one to ask if building larger surveys is justified in terms of advancing dark energy knowledge.

In Fig. 3 we plot the dark energy Figure-of-Merit for a number of ground-based surveys – CFHT, VST-KIDS, Pan-STARRS (PS1), HyperSuprimeCam (HSC), darkCAM, Dark Energy Survey (DES), WFOS and LSST – as a function of expected completion date. We have combined all of the surveys with Planck which is due to have results by 2010. The CFHTLS, VST-KIDS, darkCAM, DES and LSST are lensing surveys and both the 3-D shear power and 3-D geometric shear-ratio methods have been applied, combined with a BAO analysis using photometric redshifts. The HSC+WFOS5000 is a combined weak lensing and spectroscopic BAO survey over 5000 sq. degs. with a CMB prior.

We can conclude from Fig. 3 that the information gained from future surveys will not saturate. In an ideal world the dark energy Figure-of-Merit is expected to halve every 2.5 years, i.e., there is an exponential growth in information about dark energy with time. Clearly the information gained about dark energy is data-limited for the foreseeable future, and will grow with the increase in data-size. It will be interesting to re-visit this prediction over the next ten years to see how well surveys have kept up.

5. Summary and Conclusions

In this proceedings we have used a Fisher Information Matrix analysis to study the expected gain in information about dark energy from the CMB, 3-D weak shear power and 3-D geometric shear-ratio methods, and Baryon Acoustic Oscillation experiments. We have argued that on their own each experiment is limited in how well it can probe dark energy, but rather carves out a thin sheet in multi-parameter space and probe the dark energy at different redshifts. By combining experiments we can break these degeneracies. Combining pairs reduces the errors to $\Delta w_0 \sim 0.07$ and $\Delta w_a \sim 0.2$ with $FoM \sim 2 \times 10^{-2}$. Combining triples yields $FoM \sim 2 \times 10^{-3}$ and combining all four gives $FoM = 1.0 \times 10^{-3}$ at $z = 0.4$. We have highlighted the problem of probing dark energy at redshifts higher than $z = 1$. Finally, we have gazed into the crystal ball and tried to see with what accuracy we can potentially measure dark energy over time, as new surveys come online. Here we find that dark energy analysis will be data-limited for the foreseeable future, the rate of knowledge growing exponentially with time as the size of data-sets grows. Despite this there is much still missing from a more complete analysis, including cross-correlations between surveys, intrinsic alignments in lensing, photometric redshift bias, scale dependent bias in BAO's, nonlinearity in lensing and BAOs. But while the timescales and accuracies are most probably optimistic, this does imply dark energy science has much to learn in the next decade.

Acknowledgements: Many thanks to Alan Heavens, John Peacock, David Bacon, Bhuvnesh Jain and Masahiro Takada.

References

- Blake, C. & Glazebrook, K., 2003, ApJ, 594, 665
- Heavens, A., 2003, MNRAS, 343, 1327
- Heavens, A., Kitching, T., & Taylor, A., 2006, MNRAS, 380, 1029
- Jain, B. & Taylor, A. N., 2003, Phys. Rev. Lett, 91, 1302
- Sanchez, A., et al., 2006, MNRAS, 366, 189
- Spergel, D., et al., 2006, ApJS, 177, 377
- Reiss, A., et al., 1998, Astron.J. 116, 1009
- Taylor, A. N., et al., 2004, MNRAS, 353, 1176
- Taylor, A. N., Kitching, T., Bacon, D., & Heavens, A., 2007, MNRAS, 2007, 374, 1377
- Tegmark, M., Taylor, A. N., & Heavens, A. F., 1997, Astrophys.J., 480, 22